J|A|C|S
ARTICLES
Published on Web 01/10/2006

A Structural Investigation of the N−B Interaction in an *o*-(*N*,*N*-Dialkylaminomethyl)arylboronate System

Lei Zhu, Shagufta H. Shabbir, Mark Gray, Vincent M. Lynch, Steven Sorey, and Eric V. Anslyn*

Contribution from the Department of Chemistry and Biochemistry, The University of Texas at Austin, Austin, Texas 78712

Received August 24, 2005; E-mail: anslyn@ccwf.cc.utexas.edu

Abstract: *o*-(Pyrrolidinylmethyl)phenylboronic acid (**4**) and its complexes with bifunctional substrates such as catechol, α-hydroxyisobutyric acid, and hydrobenzoin have been studied in detail by X-ray crystallography, ^{11}B NMR, and computational analysis. The N−B interactions in analogous boronic acids and esters have been extensively cited in molecular recognition and chemosensing literature. The focal point of this study was to determine the factors that are pertinent to the formation of an intramolecular N−B dative bond. Our structural study predicts that the formation of an N−B dative bond, and/or solvent insertion to afford a tetrahedral boronate anion, depends on the solvent and the complexing substrate present. Specifically, from ^{11}B NMR studies, complexation of **4** with electron-withdrawing and/or vicinally bifunctionalized substrates promotes both the formation of N−B dative bonds and the solvation of sp^2 boron to a tetrahedral sp^3 boronate. In the solid state, the presence of an N−B dative bond in the complex of **4** and catechol (**7**) depends on the solvent from which it crystallizes. From chloroform, an N−B bond was observed, whereas from methanol, a methoxylated boronate was formed, where the methoxy group is hydrogen-bonded with the neighboring tertiary ammonium ion. The structural optimization of compounds **4** and **7** using density functional theory in a simulated water continuum also predicts that complexation of **4** and catechol promotes either the formation of an N−B bond or solvolysis if 1 equiv of water is present. The conclusion from this study will help in the design of future chemosensing technologies based on *o*-(*N*,*N*-dialkylaminomethyl)-arylboronate scaffolds that are targeting physiologically important substances such as saccharides, α-hydroxycarboxylates, and catecholamines.

Introduction

Since the discovery that phenylboronic acid condenses with mannitol and other polyols to form phenylboronates,[1] arylboronic acid functional groups have been incorporated into receptors for polyols and their derivatives.[2−7] Target substrates of physiological importance include saccharides, nucleosides, α-hydroxycarboxylates, and catecholamines. Over the past 50 years, sensing applications[8−26] (reviews on saccharide sensing, refs 8−14; examples on α-hydroxycarboxylates sensing, refs 15−21; examples on catacholamine sensing, refs 22−26) and chromatographic protocols[27−34] that target these molecules on the basis of their reversible covalent associations with boronic acid receptors have been created, including a few near-clinical applications.[35,36] Furthermore, some structural and mechanistic

(1) Kuivila, H. G.; Keough, A. H.; Soboczenski, E. J. *J. Org. Chem.* **1954**, *19*, 780−783.
(2) Dewar, M. J. S.; Kubba, V. P.; Pettit, R. *J. Chem. Soc., Abstracts* **1958**, 3076−3079.
(3) Lorand, J. P.; Edwards, J. O. *J. Org. Chem.* **1959**, *24*, 769−774.
(4) Letsinger, R. L.; Hamilton, S. B. *J. Org. Chem.* **1960**, *25*, 592−595.
(5) Jensen, K. A.; Pedersen, T. *Acta Chem. Scand.* **1961**, *15*, 1780−1781.
(6) Letsinger, R. L.; MacLean, D. B. *J. Am. Chem. Soc.* **1963**, *85*, 2230−2236.
(7) Kankare, J. J.; Varhiala, J. *Anal. Chim. Acta* **1978**, *99*, 151−156.
(8) James, T. D.; Linnane, P.; Shinkai, S. *Chem. Commun.* **1996**, 281−288.
(9) James, T. D.; Sandanayake, K. R. A. S.; Shinkai, S. *Angew. Chem., Int. Ed. Engl.* **1996**, *35*, 1910−1922.
(10) Wang, W.; Gao, X.; Wang, B. *Curr. Org. Chem.* **2002**, *6*, 1285−1317.
(11) Striegler, S. *Curr. Org. Chem.* **2003**, *7*, 81−102.
(12) Fang, H.; Kaur, G.; Wang, B. *J. Fluoresc.* **2004**, *14*, 481−489.
(13) Phillips, M. D.; James, T. D. *J. Fluoresc.* **2004**, *14*, 549−559.
(14) Cao, H.; Heagy, M. D. *J. Fluoresc.* **2004**, *14*, 569−584.
(15) Gray, C. W., Jr.; Houston, T. A. *J. Org. Chem.* **2002**, *67*, 5426−5428.
(16) Zhu, L.; Anslyn, E. V. *J. Am. Chem. Soc.* **2004**, *126*, 3676−3677.
(17) Wiskur, S. L.; Lavigne, J. J.; Matzger, A.; Tobey, S. L.; Lynch, V. M.; Anslyn, E. V. *Chem. Eur. J.* **2004**, *10*, 3792−3804.
(18) Nguyen, B. T.; Wiskur, S. L.; Anslyn, E. V. *Org. Lett.* **2004**, *6*, 2499−2501.
(19) Zhao, J.; Fyles, T. M.; James, T. D. *Angew. Chem., Int. Ed.* **2004**, *43*, 3461−3464.
(20) Zhao, J.; Davidson, M. G.; Mahon, M. F.; Kociok-Kohn, G.; James, T. D. *J. Am. Chem. Soc.* **2004**, *126*, 16179−16186.
(21) Zhu, L.; Zhong, Z.; Anslyn, E. V. *J. Am. Chem. Soc.* **2005**, *127*, 4260−4269.
(22) Yoon, J.; Czarnik, A. W. *Bioorg. Med. Chem.* **1993**, *1*, 267−271.
(23) Secor, K. E.; Glass, T. E. *Org. Lett.* **2004**, *6*, 3727−3730.
(24) Maue, M.; Schrader, T. *Angew. Chem., Int. Ed.* **2005**, *44*, 2265−2270.
(25) Paugam, M.-F.; Valencia, L. S.; Boggess, B.; Smith, B. D. *J. Am. Chem. Soc.* **1994**, *116*, 11203−11204.
(26) Paugam, M.-F.; Bien, J. T.; Smith, B. D.; Chrisstoffels, L. A. J.; de Jong, F.; Reinhoudt, D. N. *J. Am. Chem. Soc.* **1996**, *118*, 9820−9825.
(27) Weith, H. L.; Wiebers, J. L.; Gilham, P. T. *Biochemistry* **1970**, *9*, 4396−4401.
(28) Rosenberg, M.; Wiebers, J. L.; Gilham, P. T. *Biochemistry* **1972**, *11*, 3623−3628.
(29) Barker, S. A.; Hatt, B. W.; Somers, P. J.; Woodbury, R. R. *Carbohydr. Res.* **1973**, *26*, 55−64.
(30) Reske, K.; Schott, H. *Angew. Chem., Int. Ed. Engl.* **1973**, *12*, 417−418.
(31) Wulff, G.; Vesper, W. *J. Chromatogr.* **1978**, *167*, 171−186.
(32) Glad, M.; Ohlson, S.; Hansson, L.; Mansson, M.-O.; Mosbach, K. *J. Chromatogr.* **1980**, *200*, 254−260.
(33) Wulff, G. *Pure Appl. Chem.* **1982**, *54*, 2093−2102.
(34) Wulff, G. *Angew. Chem., Int. Ed. Engl.* **1995**, *34*, 1812−1832.

10.1021/ja055817c CCC: $33.50

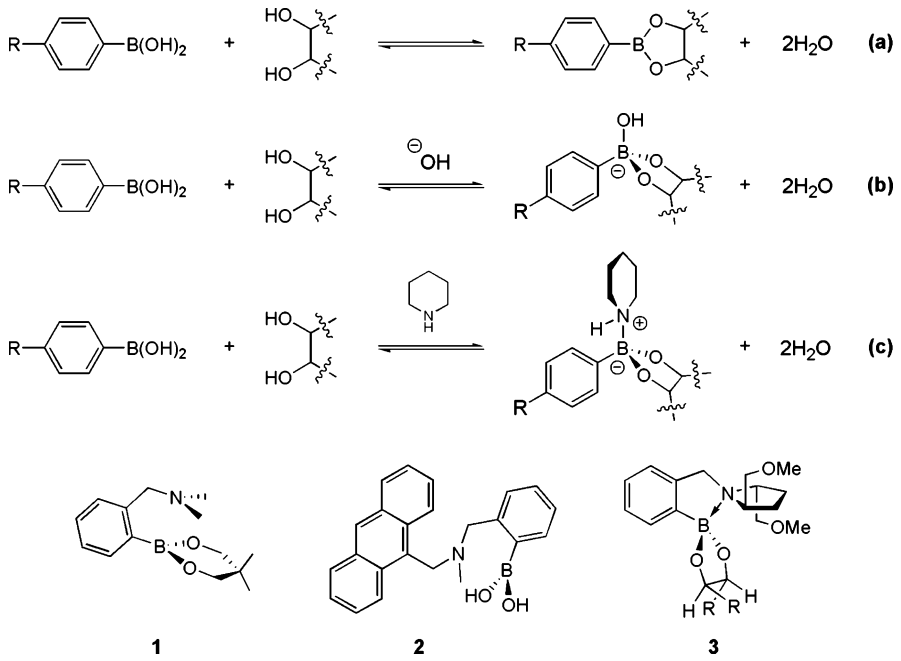

Figure 1. (a) Reversible association between an arylboronic acid and a vicinal diol. (b) Arylboronic acid and vicinal diol association under alkaline conditions. (c) Arylboronic acid and vicinal diol association in the presence of piperidine. Compounds **1**−**3** are examples of phenylboronates with *o*-(*N*,*N*-dialkylaminomethyl) groups. An N−B dative bond is shown in compound **3**.[21]

understanding of this important reversible covalent association has been gained.[37−50]

Early studies of arylboronic acid/diol association and arylboronic ester exchange reactions showed that the equilibrium (Figure 1a) becomes rapid when the reactions proceed in aqueous alkaline solutions (Figure 1b) or in the presence of certain nitrogenous bases such as piperidine (Figure 1c).[31,40] [Fluoride (F^-) was also found to facilitate boronic ester formation; see refs 51 and 52.] Further investigations using boronic acids or esters with covalently appended neighboring nitrogenous groups (one of the earliest examples is compound **1**)[38] confirmed the previous findings,[38,39] where the N−B interactions were implicated in the acceleration effect.

Eleven years ago, Shinkai et al. published a landmark study on saccharide sensing using the fluorescent boronic acid receptor **2**.[53] It was postulated that the N−B coordination in **2** is enhanced upon association with saccharide substrates. This enhanced coordination arrests the photoinduced electron transfer (PET) process from the tertiary amino group to the anthracenyl fluorophore. Hence, the fluorescence of **2** is turned on in the presence of saccharide molecules in aqueous media.[8,9,54] In the following years, beautiful elaborations on the basic design embodied in **2** have emerged for tuning selectivity and sensitivity, and such examples are generally seen as crowning achievements in the field of chemosensing.[8−14]

Recently, data from Wang's group suggested that N−B dative bonds may not be present in the boronate esters formed between *o*-aminomethylphenylboronic acids and saccharide molecules in aqueous media due to the competing solvolysis process (B in Figure 2).[49,55] By analyzing the pH profiles of compound **2** and its complexes, considering the fluorescence intensity variations upon association with different saccharide molecules (including fructose and sorbitol that bind to boronic acids trivalently to preclude N−B bond formation), and performing a computational analysis of the N−B bond strengths, Wang et al. concluded that the alternative solvent insertion pathway should be operative in aqueous media, and that strengthened solvolysis may be the cause of the fluorescence modulation of compound **2** upon association with saccharide molecules.

The question regarding N−B coordination in *o*-(*N*,*N*-dialkylaminomethyl)phenylboronate derivatives attracted our attention because we were exploring chiral molecules that have reasonable structural rigidity for enantioselective sensing of α-hydroxycarboxylates and chiral diols. In a structure such as **3** (Figure 1), the spiro arrangement around the boron atom results from formation of the N−B dative bond and should give a significant

(35) Suri, J. T.; Cordes, D. B.; Capuccio, F. E.; Wessling, R. A.; Singaram, B. *Angew. Chem., Int. Ed.* **2003**, *42*, 5857−5859.
(36) Badugu, R.; Lakowicz, J. R.; Geddes, C. D. *Curr. Opin. Biotechnol.* **2005**, *16*, 100−107.
(37) Burgemeister, T.; Grobe-Einsler, R.; Grotstollen, R.; Mannschreck, A.; Wulff, G. *Chem. Ber.* **1981**, *114*, 3403−3411.
(38) Wulff, G.; Lauer, M.; Bohnke, H. *Angew. Chem., Int. Ed. Engl.* **1984**, *23*, 741−742.
(39) Lauer, M.; Bohnke, H.; Grotstollen, R.; Salehnia, M.; Wulff, G. *Chem. Ber.* **1985**, *118*, 246−260.
(40) Lauer, M.; Wulff, G. *J. Chem. Soc., Perkin Trans. 2* **1987**, 745−749.
(41) Bello-Ramirez, M. A.; Martinez, M. E. R.; Flores-Parra, A. *Heteroat. Chem.* **1993**, *4*, 613−620.
(42) Nagai, Y.; Kobayashi, K.; Toi, H.; Aoyama, Y. *Bull. Chem. Soc. Jpn.* **1993**, *66*, 2965−2971.
(43) Norrild, J. C.; Eggert, H. *J. Am. Chem. Soc.* **1995**, *117*, 1479−1484.
(44) Bielecki, M.; Eggert, H.; Norrild, J. C. *J. Chem. Soc., Perkin Trans. 2* **1999**, 449−455.
(45) Norrild, J. C. *J. Chem. Soc., Perkin Trans. 2* **2001**, 719−726.
(46) Norrild, J. C.; Søtofte, I. *J. Chem. Soc., Perkin Trans. 2* **2001**, 727−732.
(47) Wiskur, S. L.; Lavigne, J. J.; Ait-Haddou, H.; Lynch, V. M.; Chiu, Y. H.; Canary, J. W.; Anslyn, E. V. *Org. Lett.* **2001**, *3*, 1311−1314.
(48) Otsuka, H.; Uchimura, E.; Koshino, H.; Okano, T.; Kataoka, K. *J. Am. Chem. Soc.* **2003**, *125*, 3493−3502.
(49) Ni, W.; Kaur, G.; Springsteen, G.; Wang, B.; Franzen, S. *Bioorg. Chem.* **2004**, *32*, 571−581.
(50) Bosch, L. I.; Fyles, T. M.; James, T. D. *Tetrahedron* **2004**, *60*, 11175−11190.
(51) Paugam, M.-F.; Smith, B. D. *Tetrahedron Lett.* **1993**, *34*, 3723−3726.
(52) Kubo, Y.; Kobayashi, A.; Ishida, T.; Misawa, Y.; James, T. D. *Chem. Commun.* **2005**, 2846−2848.
(53) James, T. D.; Sandanayake, K. R. A. S.; Shinkai, S. *J. Chem. Soc., Chem. Commun.* **1994**, 477−478.
(54) James, T. D.; Sandanayake, K. R. A. S.; Iguchi, R.; Shinkai, S. *J. Am. Chem. Soc.* **1995**, *117*, 8982−8987.
(55) Franzen, S.; Ni, W.; Wang, B. *J. Phys. Chem. B* **2003**, *107*, 12942−12948.

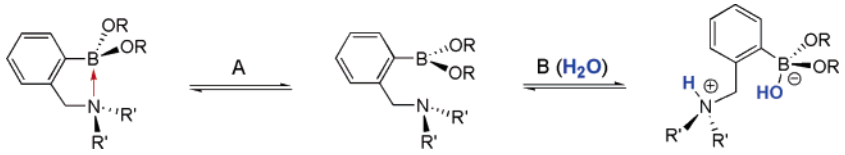

Figure 2. Three possible structures of an *o*-(*N*,*N*-dialkylaminomethyl)phenylboronic ester (or acid when R is proton).

enantioselective bias to the association of chiral substrates, such as the chiral vicinal diol (**3**) depicted in Figure 1. On the basis of this assumption, the studies on enantioselective sensing of α-hydroxycarboxylates and chiral vicinal diols were performed in aqueous media, and enantioselectivity was achieved.[16,21] To further improve the enantioselectivity of structures such as **3**, we set out on a structural study to confirm or refute the presence of the N−B bond in an *o*-(*N*,*N*-dialkylaminomethyl)phenylboronate. With this study, we wish to provide a comprehensive picture, from a structural perspective, of the reversible association between an *o*-(*N*,*N*-dialkylaminomethyl)phenylboronic acid and its substrates in protic media. Further, future sensing technology development based upon boronic acid receptors should greatly benefit from the structural details revealed in this study of this particularly important association event.

Results and Discussion

A method for the direct observation of an N−B dative bond, or the lack thereof, in an *o*-(*N*,*N*-dialkylaminomethyl)arylboronate under various experimental conditions was desired. In this study, compounds **4**−**6** were used to investigate the existence of the N−B bond, as well as the factors that modulate the characteristics of the N−B interactions. First, selected free boronic acid receptors and complexes with catechol were analyzed by X-ray crystallography; second, their solution structures were studied with ^{11}B NMR; and third, the structures of the solution species involved in the association events between compound **4** and catechol were examined by computational analysis.

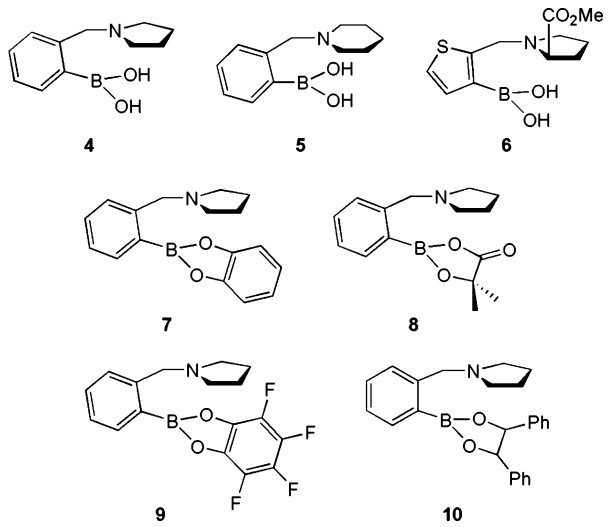

1. X-ray Crystallographic Analysis. Crystals of X-ray diffractable quality of boronic acid receptors **4**−**6**[21] were created by diffusing pentane or hexanes into concentrated solutions of chloroform. We postulated that the use of an aprotic solvent would facilitate N−B bond formation by excluding solvolysis. Compound **4** trimerizes into a cyclic anhydride to afford a six-membered-ring motif with alternating boron and oxygen atoms (Figure 3). Two of the three boron atoms (B1, B2) adopt a tetrahedral configuration with the pyrrolidinyl nitrogen atoms (N1, N2) coordinated. The lengths of the N−B bonds[56] are 1.743 and 1.744 Å, respectively, comparable to the values reported for other boronic acid molecules with similar configurations.[17,47] The other boron (B3) center adopts a trigonal planar configuration, with nitrogen atom N3 left unbound. The O1−B3−O3 angle is 121.33°, which is typical for an sp^2 hybridization. The average B3−O bond length is 1.37 Å, slightly shorter than that of B1/B2−O bonds (1.43 Å). The shorter bond length is a result of electron back-donation from oxygen to the electron-deficient sp^2 boron. Analogous trimerized cyclic boronic anhydride structures with various trigonal/tetrahedral boron atom arrangements have also been reported.[57−59] Hence, as part of the boronate anhydride, the N−B dative bond was observed.

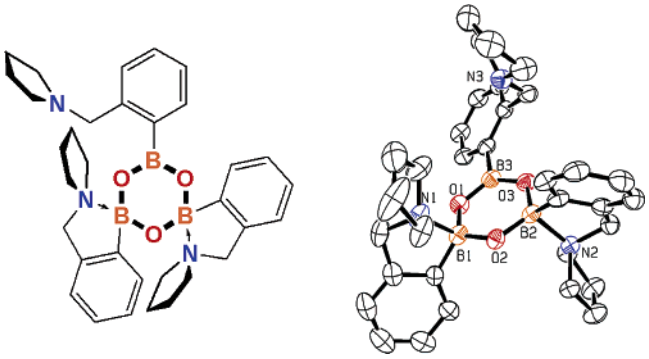

Figure 3. Left: ChemDraw presentation of the cyclic anhydride of **4**. Right: ORTEP diagrams (50% probability ellipsoids) of the cyclic anhydride of **4**. Hydrogen atoms are removed for clarity.

Compounds **5** and **6** dimerize through hydrogen bonds between the trigonal planar boronic acid moieties (Figure 4). The O−B−O bond angle is 119.56° in compound **5**, where the average B−O bond length is 1.36 Å. Such arrangement is reminiscent of solid-state carboxylic acid structures.[60] The dimers lie around their crystallographic inversion centers. The nitrogen atoms interact with the boronic hydroxyl groups through hydrogen bonds. The N−B dative bond is not observed in these two boronic acids that were crystallized from chloroform. Similar structures have also been reported in the literature.[46]

However, it should be noted that a number of similar boronic acid structures have been reported in the past decade.[17,46,47,57−59,61−63] N−B dative bonds were observed in many,

(56) Höpfl, H. *J. Organomet. Chem.* **1999**, *581*, 129−149.
(57) Norrild, J. C.; Søtofte, I. *J. Chem. Soc., Perkin Trans. 2* **2002**, 303−311.
(58) Giles, R. L.; Howard, J. A. K.; Patrick, L. G. F.; Probert, M. R.; Smith, G. E.; Whiting, A. *J. Organomet. Chem.* **2003**, *680*, 257−262.
(59) Bosch, L. I.; Mahon, M. F.; James, T. D. *Tetrahedron Lett.* **2004**, *45*, 2859−2862.
(60) Fournier, J.-H.; Maris, T.; Wuest, J. D.; Guo, W.; Galoppini, E. *J. Am. Chem. Soc.* **2003**, *125*, 1002−1006.
(61) Toyota, S.; Oki, M. *Bull. Chem. Soc. Jpn.* **1992**, *65*, 1832−1840.
(62) Toyota, S.; Futawaka, T.; Asakura, M.; Ikeda, H.; Oki, M. *Organometallics* **1998**, *17*, 4155−4163.

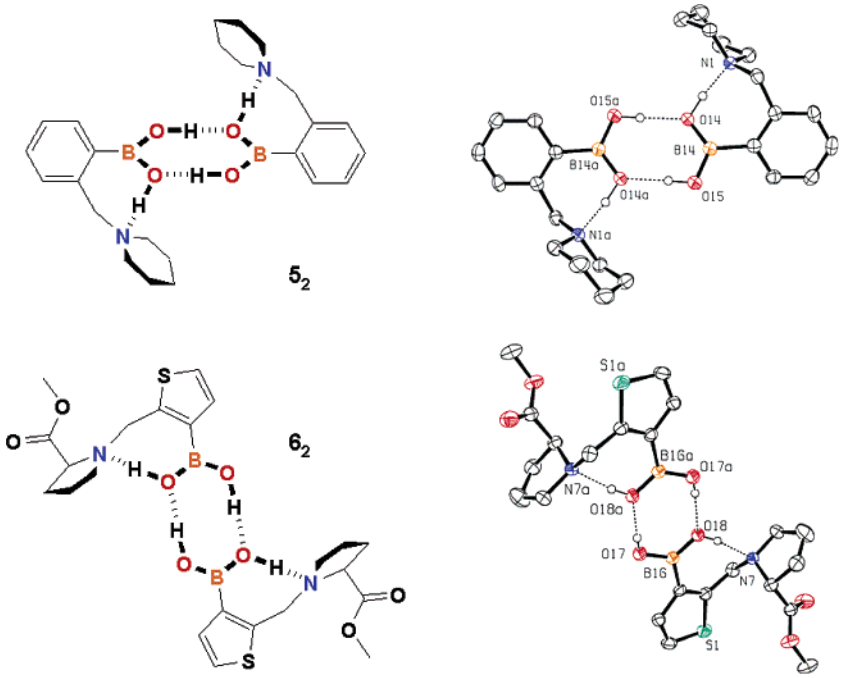

Figure 4. Left: ChemDraw presentations of the hydrogen-bonded dimers $\mathbf{5}_2$ and $\mathbf{6}_2$. Right: ORTEP diagrams (50% probability ellipsoids) of $\mathbf{5}_2$ and $\mathbf{6}_2$. Most hydrogen atoms are removed for clarity.

but not all, cases when such structures were obtained through crystallization from aprotic solvents.[47,57−59,61,62] Solution structural characterization of similar compounds in aprotic solvents also unequivocally showed the existence of N−B dative bonds.[37,56] Therefore, it is well established that in aprotic solvents, when a solvolysis pathway is absent, N−B coordination is commonly, but not exclusively, observed. Our findings show that the presence or absence of the N−B bond is a balance of many forces, of which crystal packing can likely have a significant effect.

The N−B bond formation in aprotic solvents is further corroborated by the structure of **7**, the complex between compound **4** and catechol. Complex **7** was prepared by mixing equal molar parts of **4** and catechol in chloroform, followed by azeotropic removal of water. The product was recrystallized by diffusing pentane into a concentrated chloroform solution.[64] In the single-crystal structure, two different isoforms were found (Figure 5A, one isoform is shown), differing in conformations of the pyrrolidinyl ring. In both, the nitrogen atom is coordinated with boron. The N−B bond lengths in the conformers are 1.683 and 1.700 Å, respectively. They are slightly shorter than observed in the trimeric structure of **4**, suggesting strengthened N−B interactions. The O−B−O bond angle is 105.70°, typical of a tetrahedral geometry. The average B−O bond length is 1.47 Å, significantly longer than that observed in compounds **4**−**6** with sp^2 boron atoms. The observation of an N−B bond is also consistent with the chronicled structural studies by ^{1}H, ^{11}B, and ^{15}N NMR on boronic acids with neighboring amino groups and diol complexes in aprotic solvents ($CDCl_3$, CD_2Cl_2).[37−40,65−67]

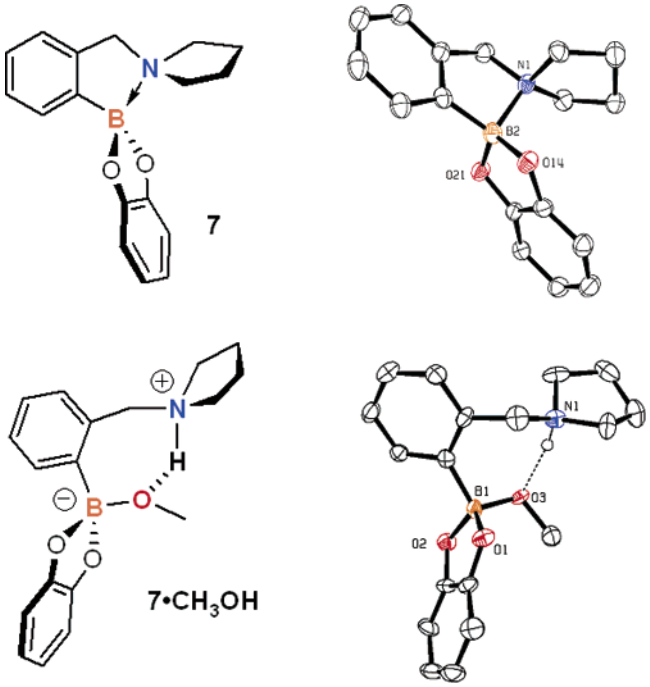

Figure 5. Left: ChemDraw presentations of the complexes (**7** and **7**•CH_3OH) between **4** and catechol. Right: ORTEP diagrams (50% probability ellipsoids) of arbitrary conformers of **7** and **7**•CH_3OH. Most hydrogen atoms are removed for clarity.

When complex **7** was crystallized from methanol, a protic solvent, instead of an N−B dative bond, the boron atom was coordinated with a methoxy group from the solvent, and the nitrogen atom was protonated (Figure 5B). Three conformers were observed in the crystal lattice. They differ slightly in their pyrrolidinyl ring conformations. The average B−O bond length is 1.50 Å, and the O−B−O bond angle of the cyclic catechol

(63) Braga, D.; Polito, M.; Bracaccini, M.; D'Addario, D.; Tagliavini, E.; Sturba, L. *Organometallics* **2003**, *22*, 2142−2150.
(64) The hygroscopicity of complex **9** is evident from comparing the ^{1}H NMR ($CDCl_3$) spectra of fresh and aged samples. The aged sample can be restored with an azeotropic treatment.
(65) Biedrzycki, M.; Scouten, W. H.; Biedrzycka, Z. *J. Organomet. Chem.* **1992**, *431*, 255−270.
(66) Lauer, M.; Wulff, G. *J. Organomet. Chem.* **1983**, *256*, 1−9.
(67) Brown, H. C.; Vara Prasad, J. V. N. *J. Org. Chem.* **1986**, *51*, 4526−4530.

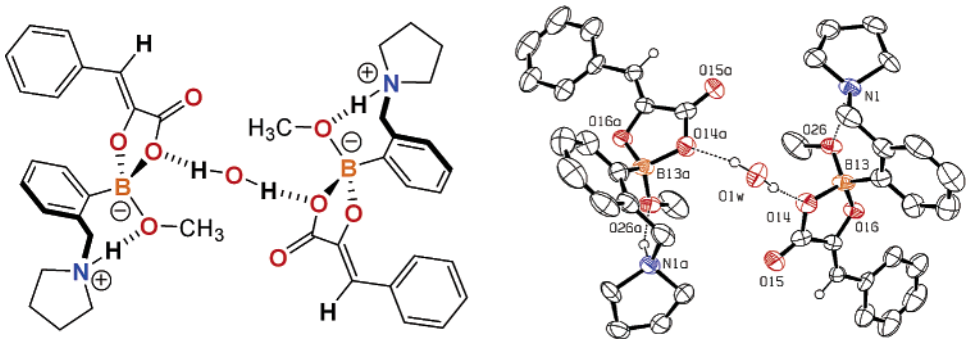

Figure 6. Left: ChemDraw presentation of a dimer of the complex between **4** and phenylpyruvic acid bridged via a water molecule. Right: ORTEP diagram (50% probability ellipsoids) of the hydrogen-bonded dimer of the complex. Most hydrogen atoms have been removed for clarity.

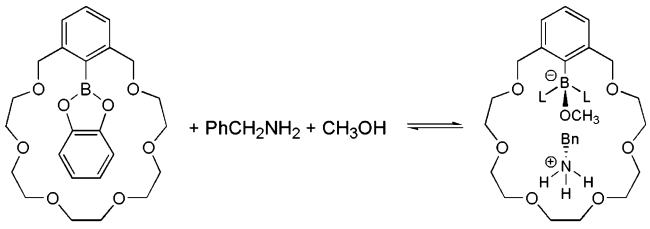

Figure 7. Formation of zwitterionic amino boronate **12** as reported by Reetz et al.

boronate is 102.43°. In all the conformers, the nitrogen and boron atoms are associated through hydrogen bonds between N−H and B−OCH_3. A similar N−B interaction, based upon hydrogen bonding rather than N−B coordination, was also observed in the structure of the boronate ester between **4** and phenylpyruvic acid (Figure 6). This structure was also obtained through crystallization from methanol. The carbonyl group is enolized to afford a vicinal dihydroxyl moiety that forms a cyclic ester with compound **4**.[21] The complex dimerizes through a water molecule lying on a crystallographic 2-fold rotation axis at $0,y,{}^1/_4$. The B−OCH_3 and pyrrolidinyl N−H are associated via hydrogen bonds.

Zwitterionic ammonium boronate structures have been reported previously. Reetz et al. prepared a crown ether phenyl boronate of catechol (**11**, Figure 7).[68,69] When compound **11** was allowed to react with a 1:1 mixture of methanol and benzylamine in dichloromethane, a ternary complex (**12**) was formed. The crystal structure showed that methanol was deprotonated by benzylamine in this ternary complex and the methoxy group was coordinated with the boronate to afford a zwitterionic complex.[69] The ammonium ion was stabilized by both hydrogen bonding with the crown ether moiety and ion pairing with the boronate anion. As in the structures in Figures 5 and 6, the amino group in compound **12** forms an ammonium ion instead of coordinating with the boron atom. The substantial stabilization of the ammonium ion by a crown ether moiety apparently facilitates the zwitterion formation.

On the other hand, N−B bonded amino boronate has also been crystallized from protic solvents. We previously reported a crystal structure of *o*-(*N*-benzylaminomethyl)phenylboronic acid (**13**) obtained from methanol as a dimethyl boronate with an N−B bond of 1.665 Å (Figure 8).[17] The shortened N−B bond length, compared to that of **7**, suggests stronger N−B coordination. The strengthened N−B interaction should be due to the more sterically accessible nitrogen lone pair of electrons in a secondary amine than in a tertiary amine as in **7**. In support of this, steric hindrance has been invoked by Norrild et al. as the cause for the absence of an N−B bond in a ferrocene bisboronic acid complex with D-sorbitol.[46] Interestingly, the ^{11}B NMR−pH profile of **13** in 10% CD_3OD in water indicates that the boron atom is solvated in solution (see the next section).[47] Therefore, as evidenced by the discrepancy between the structures of compound **13** in solid state and in solution, caution should be applied when solution behavior is predicted based upon solid-state evidence.

Further evidence for steric effects comes from Reetz. He reported a catechol phenylboronate structure with an N−B coordinating benzylamine.[70] The coordination of boron with this primary amine affords an N−B bond length of 1.612 Å, shorter than that in compound **13**. The ^{11}B NMR chemical shift of the benzylamine complex in CD_2Cl_2 is 9 ppm, indicating a stronger sp^3 character of boron than that of the tertiary amino group-based compounds reported in this article, whose ^{11}B NMR chemical shifts range from 12 to 16 ppm (see the next section). Therefore, the balance between N−B coordination and the solvated analogue is also influenced by steric interactions, likely favoring N−B coordination with primary amines and smaller alkyl groups, in both solution and solid states.

Therefore, the conclusion drawn from the X-ray crystallographic analysis is that the formation of either N−B coordinated or solvated structures largely depends on the solvent from which a boronate crystallizes.

2. ^{11}B NMR Analysis. 2.1. Structural Characterization in Solution. Structural studies using ^{11}B NMR were carried out to investigate the factors (e.g., solvent, pH) that affect the nature of the N−B interaction in solution. The same sample of crystals used to obtain the X-ray structure of **4** displays two ^{11}B signals at 26.8 and 15.7 ppm in $CDCl_3$ (Figure S1, Supporting Information; Table 1). The major signal, accounting for ~66% of the sample, at 15.7 ppm is assigned to the N−B coordinated tetrahedral boron on the basis of comparison with literature data.[37,38,71] The minor signal (~34%) at 26.8 ppm is assigned to the trigonal planar boron species with no N−B bond. The relative abundance of the tetrahedral and trigonal planar boron species (roughly 2:1) correlates well to what was observed in the single-crystal structure of the cyclic trianhydride (Figure

(68) Reetz, M. T.; Niemeyer, C. M.; Harms, K. *Angew. Chem., Int. Ed. Engl.* **1991**, *30*, 1472−1474.
(69) Reetz, M. T.; Niemeyer, C. M.; Harms, K. *Angew. Chem., Int. Ed. Engl.* **1991**, *30*, 1474−1476.
(70) Reetz, M. T.; Niemeyer, C. M.; Hermes, M.; Goddard, R. *Angew. Chem., Int. Ed. Engl.* **1992**, *31*, 1017−1019.
(71) Arimori, S.; Ward, C. J.; James, T. D. *Chem. Commun.* **2001**, 2018−2019.

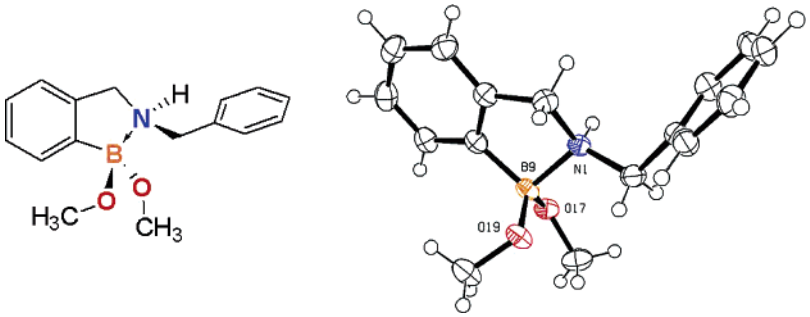

Figure 8. ChemDraw presentation and crystal structure (ORTEP, 50% probability ellipsoids) of dimethyl *o*-(*N*-benzylaminomethyl)phenylboronate (**13**).

Table 1. ^{11}B NMR Chemical Shifts of Selected Boronic Acids and Esters in $CDCl_3$ and CD_3OD, Respectively[a]

	^{11}B NMR (δ/ppm, 160 MHz)	
compd	in $CDCl_3$	in CD_3OD
4	26.8, 15.7*	8.3
5	29.2	5.4
7	14.7*, 10.4	14.3, 10.2*, 8.2
8	12.0*, 7.8	8.0
9	15.5*, 11.6	11.8*, 8.1
10	13.2	9.0
11[68]	30 (in CD_2Cl_2)	ND
12[69]	9.0 (in CD_2Cl_2)	ND
13[17]	ND	10.3

[a] All ^{11}B NMR chemical shifts are referred to external standard BF_3-OEt_2. Major signals are indicated with an asterisk. ND, not determined.

3). In CD_3OD, however, the same set of crystals of compound **4** shows a single peak at 8.3 ppm. This signal, which is significantly upfield from the resonance of the N−B coordinated species, is assigned to the fully solvated species,[72] analogous to other literature reports.[42,47,48,73] The difference of ^{11}B NMR data of compound **4** with respect to NMR solvents suggests that the boron center is very prone to solvolysis, which is in agreement to the conclusion drawn from the solid-state studies.

In the ^{11}B NMR spectrum of complex **7** in $CDCl_3$ (Figure S3, Supporting Information), the signal at 26.8 ppm found for the cyclic trimer of **4** disappears, indicating that the boron atom completely adopts a tetrahedral configuration upon associating with catechol. The major signal (∼90%) at 14.7 ppm is assigned to the N−B coordinated species. The minor signal (∼10%) at 10.4 ppm is assigned to the solvated species. The small extent of solvent insertion is attributed to the adventitious wetting of $CDCl_3$. The assignment of the solvated species is based on the spectrum of complex **7** in CD_3OD (Figure S4, Supporting Information), in which the major signal (∼80%) of **7** appears at 10.2 ppm. Also in CD_3OD, a minor peak at 14.3 ppm (∼10%) was observed, which is indicative of a small portion of N−B coordinated species. Another minor species (∼10%) was observed at 8.2 ppm, which is assigned to the solvated compound **4** from the dynamic dissociation of the complex **7** to **4** and catechol in CD_3OD. The ^{11}B NMR assignments of different species are summarized in Figure 9A.

The solvent-dependent ^{11}B NMR spectra of compounds **4** and **7** was in agreement with the solid-state structural studies — the boron atom in this particular phenylboronate system is very prone to solvent insertion. In the aprotic solvent chloroform, the boron atom in free receptor **4** adopts N−B coordinated tetrahedral and/or N−B uncoordinated trigonal planar configurations. When compound **4** is associated with catechol to afford complex **7**, the complete formation of an N−B dative bond was observed (Figure 9B). The conversion of the boron hybridization state from sp^2 to sp^3 was attributed to the increased electrophilicity of the boron atom upon association. Two factors contribute to the increased electrophilicity of the boron atom: (1) the electronic induction effect from the electron-withdrawing substrate catechol and (2) the geometrical constraints to be tetrahedral upon associating with the vicinally bifunctionalized catechol molecule. In a protic solvent such as methanol, however, solvent insertion appears to be the dominant pathway for both free receptor **4** and complex **7** (Figure 9C). The boronate anion is stabilized by the proximal tertiary ammonium ion.

2.2. ^{11}B NMR Titrations in Aprotic and Protic Media. ^{11}B NMR titrations were performed to investigate the correlation between the N−B bond strength and complex formation between **4** and substrates hydrobenzoin, catechol, and α-hydroxyisobutyric acid. These three molecules model three groups of physiologically important substances — saccharides, catecholamines, and α-hydroxycarboxylates — that are common targets of boronic acid-based chemosensing applications. From the titration experiments, we wished to explore the modulation of N−B interactions in compound **4** upon association with the aforementioned substrates under different experimental conditions and to further elucidate the underlying chemical events taking place upon association.

With the addition of hydrobenzoin (either enantiomer) in $CDCl_3$, the chemical shifts of boronic acid **4** (26.7 ppm and minor at 9.3 ppm from adventitiously hydrated **4**)[74] disappeared and a peak at 13.2 ppm, which is characteristic of a nitrogen-coordinated arylboronate, developed (Figure 10A). This titration clearly shows that, in the aprotic solvent $CDCl_3$, the complex formation promotes the N−B coordination by raising the electrophilicity, or the Lewis acidity, of the boron atom. The Lewis acid−base interaction between the boronate and the tertiary amino group is strengthened as a result of complexation.

The ^{11}B NMR titration in CD_3OD started with fully solvated compound **4** at 8.1 ppm (Figure 10B). This signal disappeared with concurrent appearance of a new signal at 9.0 ppm with the addition of hydrobenzoin. The peak at 9.1 ppm was assigned to the solvated complex **10**. No N−B coordinated species was observed. The ^{11}B NMR titration experiments in both $CDCl_3$

(72) Zhong, S.; Jordan, F.; Kettner, C.; Polgar, L. *J. Am. Chem. Soc.* **1991**, *113*, 9429−9435.
(73) Singhal, R. P.; Ramamurthy, B.; Govindraj, N.; Sarwar, Y. *J. Chromatogr.* **1991**, *543*, 17−38.
(74) The spectrum differs from the one reported in Table 1, likely due to different aggregation state resulting from the difference in sample preparations. The chemical shift at 9.3 ppm is assigned to the hydrated species, whereas the chemical shift at 8.3 ppm observed in CD_3OD is assigned to the trimethyl ester of **4**.

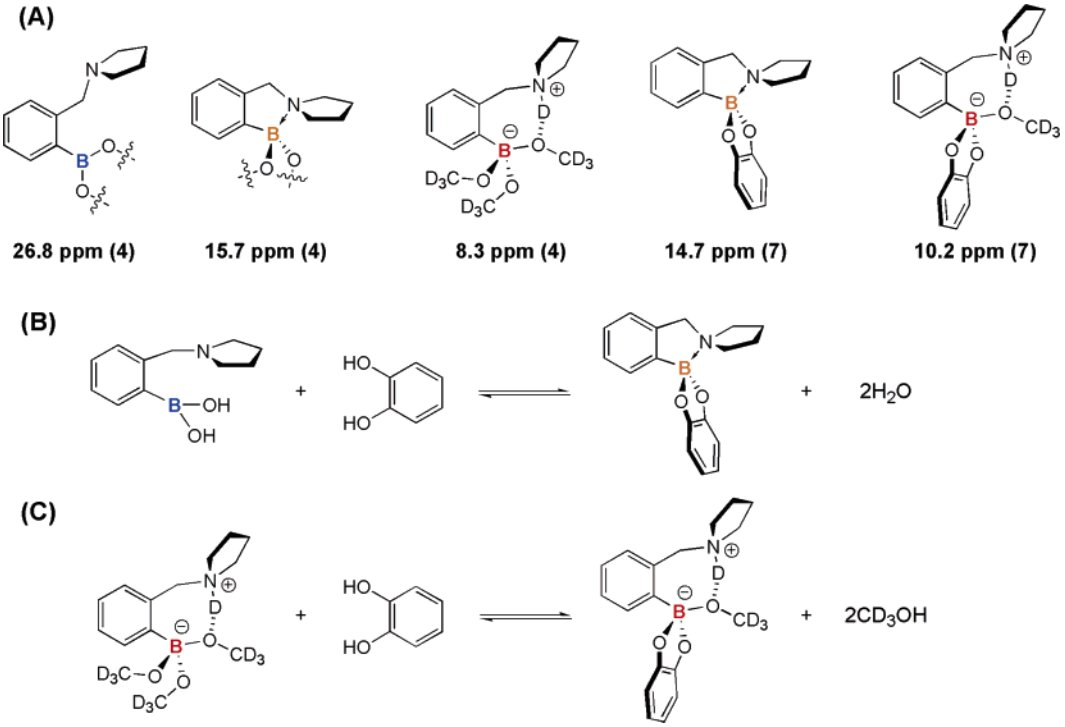

Figure 9. (A) ^{11}B NMR assignments for different species in the equilibrium between **4** and **7** (blue, trigonal planar boron; orange, tetrahedral boron with an N−B dative bond; red, tetrahedral boronate anion). (B) Reversible association between **4** and catechol in $CDCl_3$ to create **7**. (C) Reversible association between **4** and catechol in CD_3OD to create **7**·CD_3OD.

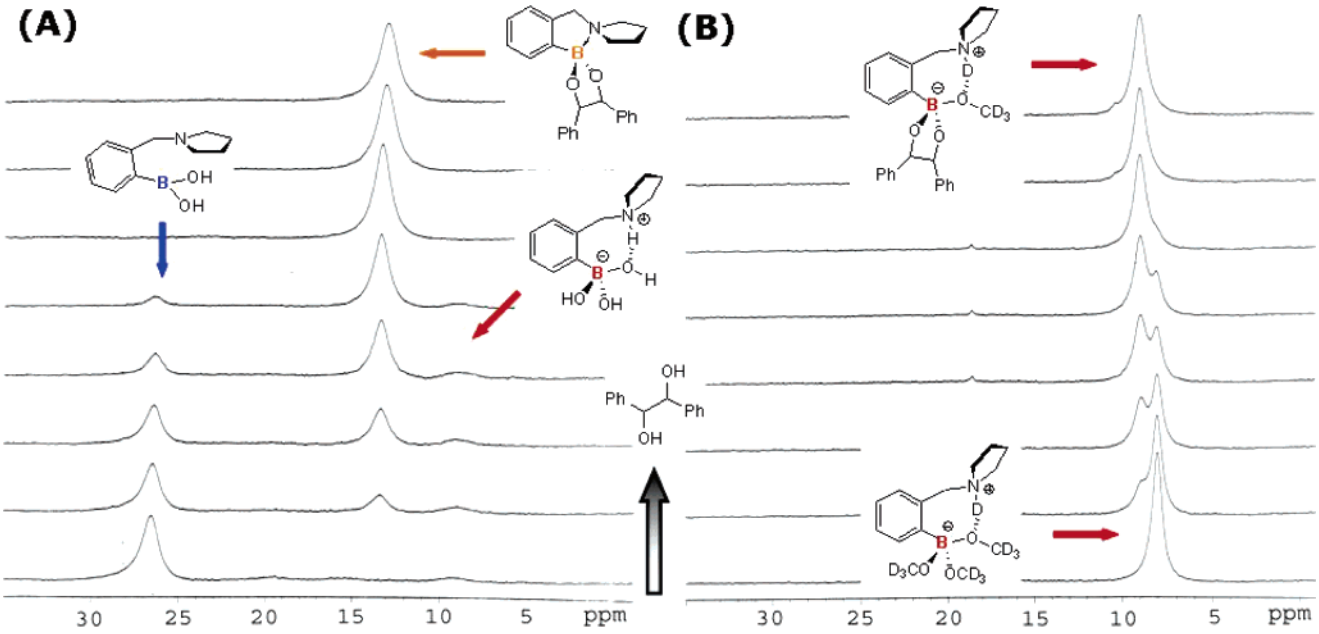

Figure 10. ^{11}B NMR spectra of compound **4** (10 mM) in the presence of 0−80 mM hydrobenzoin in $CDCl_3$ (A) and CD_3OD (B), respectively. The tiny signal at 19 ppm in (B) is from the noninterfering impurity boric acid. In (A), the free boronic acid **4** in $CDCl_3$ exists as a mixture of different aggregates, e.g., cyclic trianhydride in Figure 3.

and CD_3OD support the conclusion that the complexation to form a five-membered-ring boronate increases the electrophilicity (or Lewis acidity) of the boronate, which leads to N−B coordination in aprotic solvents. On the other hand, the solvent insertion pathway is too dominant in protic solvents such as methanol for N−B coordination to occur to a significant extent in the complex of **4** and hydrobenzoin.

Catechol behaves similarly to hydrobenzoin as a substrate of **4** in a ^{11}B NMR titration experiment in $CDCl_3$ (Figure 11A). The signals of compound **4** (mixture of aggregates) at 26.7 and 9.2 ppm were reduced while the signal of the N−B coordinated complex (**7**) at 14.8 ppm grew in upon the addition of catechol. Interestingly, when the addition of catechol was over 1 equiv, a new signal at 10.4 ppm appeared, which was assigned to a boronate triester species of a 1:2 complex. The underlying chemical event is that the Brønsted basicity of the nitrogen atom in **7** is less than that of **4** due to the strengthened N−B dative bond, the nature of which is a Lewis acid/base interaction. At

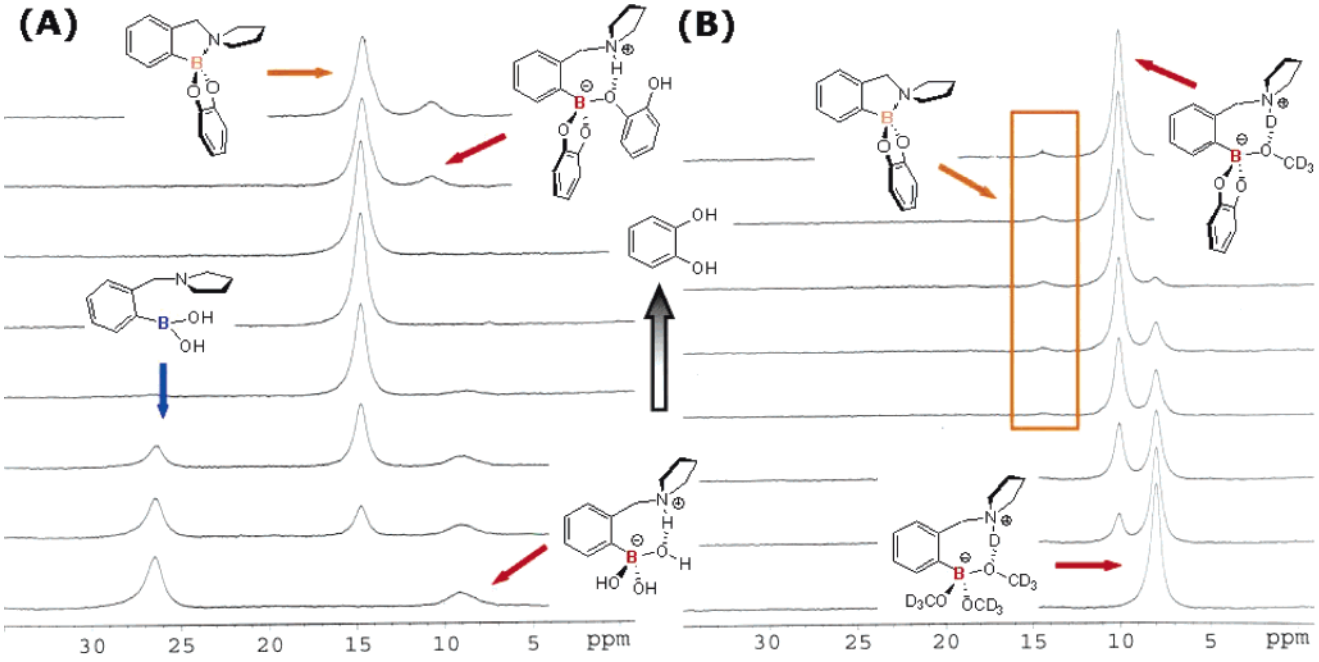

Figure 11. ^{11}B NMR spectra of compound **4** (10 mM) in the presence of 0−80 mM catechol to create complex **7** in $CDCl_3$ (A) and CD_3OD (B), respectively.

the beginning of the titration, adventitious water in the NMR solvent ($CDCl_3$) was able to protonate a small percentage of free receptor **4** (9.2 ppm). With an increasing amount of catechol, N−B coordinated complex **7** was formed and the Brønsted basicity of the nitrogen atom in **4** was consequently lowered. Therefore, the miniscule amount of water was no longer acidic enough to give a detectable amount of solvated complex. However, when the catechol exceeded 1 equiv, it acted as a Brønsted acid (pK_a 9.3)[75] that was strong enough to protonate the nitrogen atom. The resulting ammonium ion facilitated the coordination of a second catechol molecule to compound **7** to afford the anionic triester species. This situation with excess of protic substrate catechol in $CDCl_3$ simulates the solvent insertion taking place in a protic solvent.

The ^{11}B NMR titration with catechol in CD_3OD (Figure 11B) was similar to that of hydrobenzoin, except that, in addition to the solvated complex (10.3 ppm), a minor signal at 14.5 ppm also grew in with the addition of catechol. This peak was assigned to the N−B coordinated species by comparing the spectra in CD_3OD with previous characterization data of complex **7** and titration data in $CDCl_3$. Hence, the N−B coordinated and solvated species are found to be in equilibrium in this particular case. Therefore, although the solvent insertion pathway is dominant in protic solvents, the N−B coordinated species can exist in equilibrium, and its extent of formation is dependent on the particular receptor and substrate structures. In fact, Norrild et al. examined an analogue of **2** containing two boronic acid moieties and its complexation with glucose. They concluded that, in this particular case, the solvent insertion and N−B containing structures both exist within the same complex in protic media.[44]

Finally, the ^{11}B NMR titration with α-hydroxyisobutyric acid was examined (Figure 12A). In $CDCl_3$, N−B bond formation occurred with the addition of α-hydroxyisobutyric acid to compound **4** to afford the N−B coordinated complex **8** (12.1 ppm). When the α-hydroxyisobutyric acid exceeded 1 equiv, the triester species of the 1:2 complex (9.0 ppm) was observed as in the catechol case, but on a much larger scale. α-Hydroxyisobutyric acid is a much stronger Brønsted acid than both catechol and hydrobenzoin. It is able to protonate the pyrrolidinyl nitrogen of complex **8** completely, greatly favoring the formation of the anionic triester boronate. In CD_3OD (Figure 12B), the peaks of solvated receptor **4** and complex **8** coincided at 8.1 ppm. The diastereotopic methyl groups in the ^{1}H NMR of complex **8** in CD_3OD confirmed that the complex was formed in methanol. However, the existence of the N−B coordinated species was difficult to substantiate, because an exceedingly small bump at the proper ppm does grow in, but its level is so close to the background resonance of the experiment that our confidence in its existence is marginal (examine Figure 12B at the 12−13 ppm region).

2.3. ^{11}B NMR−pH Profiles. ^{11}B NMR−pH profiles of compound **4** and complex **7** in a 3:1 CH_3OH:H_2O solvent mixture were studied in an effort to characterize the solution species at various pH values. As shown in Figure 13, the first pK_a (pK_{a1}) could be either from deprotonation of the ammonium ion if the deprotonated species has the N−B dative bond or from hydroxylation of the sp^2 boron. Because there is a rapidly established equilibrium between the N−B coordinated and the solvated species, it cannot be determined from direct examination of the ^{11}B NMR spectra which structure is formed after the first deprotonation (Figure 14A). However, according to literature data, the second deprotonation of an *o*-(*N*,*N*-dialkylaminomethyl)phenylboronic acid should occur after pH 9.[45,47,54] From the ^{11}B NMR−pH profile of **4**, no chemical shift transition was observed after pH 7, where the solvated species is dominant if not exclusive (Figure 14A). Therefore, the second pK_a should not be associated with hydroxylation of the sp^2 boron. It is therefore concluded that the first deprotonation event for compound **4** is primarily the hydroxylation of the sp^2 boron, where the ^{11}B chemical shift transition from sp^2 to sp^3 was observed around pH 6.5, the value of pK_{a1}. Hence, the second

(75) Yan, J.; Springsteen, G.; Deeter, S.; Wang, B. *Tetrahedron* **2004**, *60*, 11205−11209.

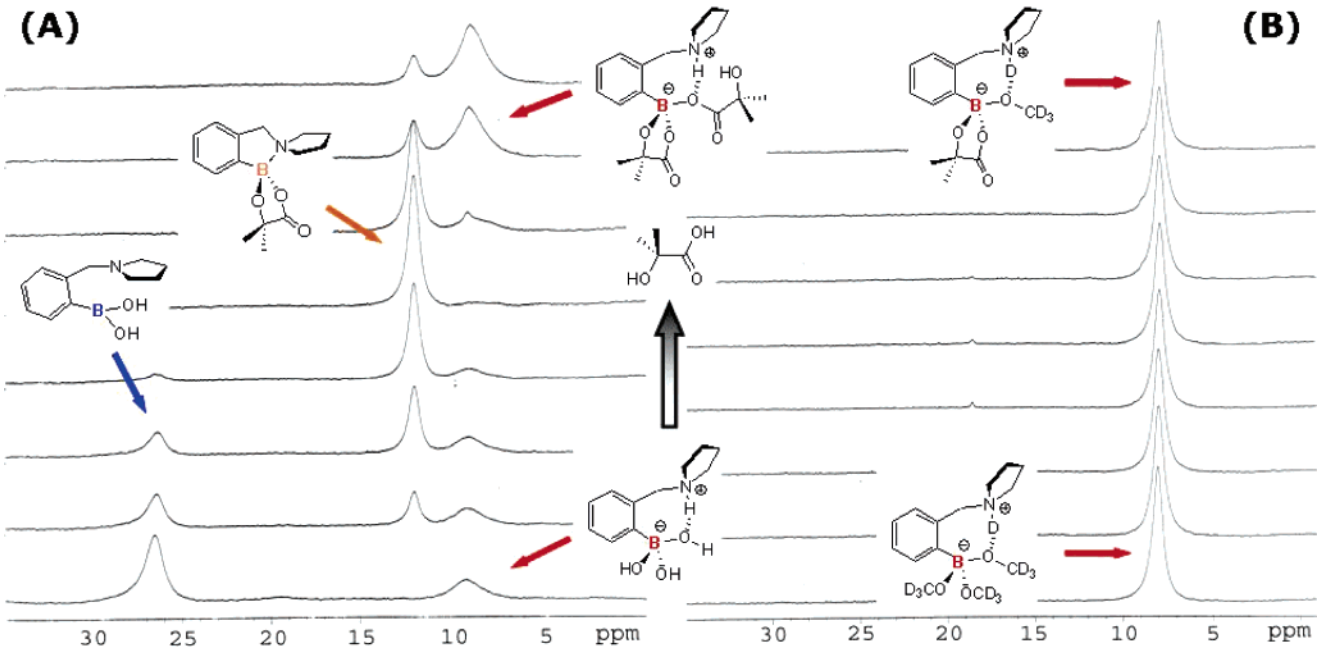

Figure 12. ^{11}B NMR spectra of compound **4** (10 mM) in the presence of 0−80 mM α-hydroxyisobutyric acid to afford complex **8** in $CDCl_3$ (A) and CD_3OD (B), respectively. The tiny signal at 19 ppm in (B) is from the noninterfering impurity boric acid. However, a signal at 12−13 ppm appears to grow in during the upper spectra of part (B), possibly indicative of an N−B species in an exceedingly small fraction.

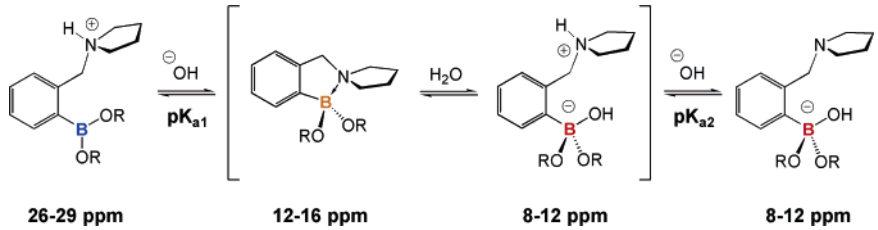

Figure 13. Deprotonation of a boronic ester in aqueous media (or acid when R = H). Different colors represent different ^{11}B NMR chemical shifts for respective species. The zwitterionic and fully deprotonated species have similar ^{11}B NMR resonances (red) due to similar chemical environments.

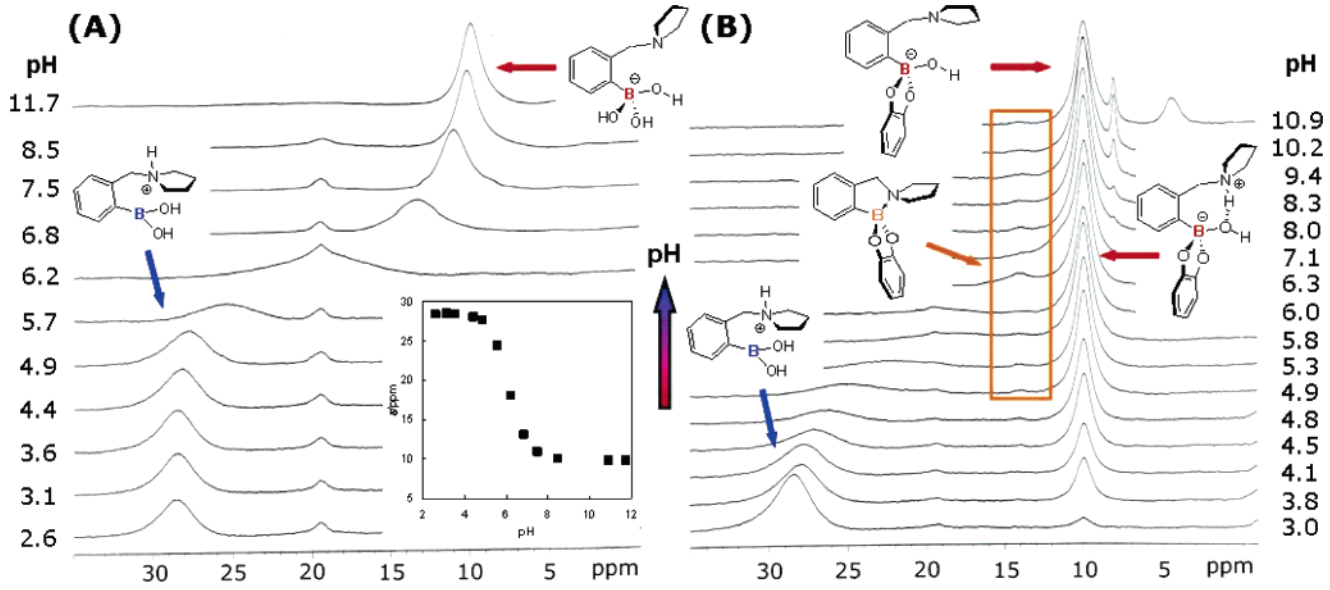

Figure 14. ^{11}B NMR spectra of compound **4** (20 mM, A) and **7** (20 mM, B) in 75% methanolic solution with HEPES (25 mM) with pH ranging from 3 to 12. The signals at 19 ppm are from the noninterfering impurity boric acid.

pK_a primarily belongs to the deprotonation of the tertiary ammonium ion, which should be at its usual range of pH 9−10,[33] or shifted slightly higher due to the proximal boronate anion. The ratio of N−B coordinated to solvated boronate dictates the extent to which each pK_a is dominated by boron solvation or ammonium deprotonation. In the cases we studied, the pK_a's are primarily attributed to the events just described above. Compared to arylboronic acids without *o*-(*N*,*N*-dialky-

laminomethyl) groups, the pK_a of the boronate is decreased by more than 3 units.[33] Such pK_a reduction is caused by the ion-pairing stabilization of the anionic sp^3 boronate from the neighboring ammonium ion.

Similar pH profiles were reported for boronic acids in previous studies from our group[47] and others.[46,50] The conclusion from our previous study on similar boronic acid molecules stated that pK_{a1} was from the deprotonation of the ammonium ion. However, this was based upon the assumption that the N−B coordinated species was dominant in solution after the first deprotonation event.[47] In light of the new experimental data that revealed the nature of the N−B interaction in protic media, we hereby conclude that pK_{a1} of compound **4** in aqueous solution is primarily from the hydroxylation of the boronate, and pK_{a2} is primarily due to the deprotonation of the tertiary ammonium ion.[33]

In the ^{11}B NMR−pH profile of complex **7** (Figure 14B), at pH 3 the boron atom in **7** was solvated to a small extent, with an sp^3 configuration (10.0 ppm). This is due to the well-known fact that the association with catechol raises the acidity of the boronate.[76−78] In other words, complex formation promotes solvolysis. However, under such acidic conditions, the affinity between **4** and catechol is low, and most of the complex is dissociated to **4** and catechol, with the boron in **4** having a trigonal planar geometry (∼27 ppm).[45,79] With increasing pH, the signal of solvated complex **7** increased, with concurrent disappearance of the chemical shift of **4**, suggesting enhanced affinity. When the pH was raised to 6.3, another minor species was observed at 14.4 ppm. This minor signal was assigned to an N−B coordinated species for three reasons: (1) Its chemical shift at 14.4 ppm corresponds to the characterized N−B coordinated species (Table 1). (2) The occurrence of this signal at pH 6.3 matches well to the pH-dependent equilibrium of an N−B coordinated species in a protic medium with the solvated species. When the pH is too low, the nitrogen atom is primarily protonated; when the pH is too high, the boron atom is primarily hydroxlyated. Only when the pH is at an intermediate value can a subtle balance be achieved between Lewis acid−base and Brønsted acid−base interactions between the amino and boronate moieties (Figure 13). (3) The association between **4** and the vicinal bifunctionalized, electron-withdrawing substrate catechol stabilizes both the N−B coordinated species and the solvated species (see the next section). As a result, two separated NMR signals corresponding to these two species were observed because their interconversion is slow relative to the ^{11}B NMR time scale. For boronic acid **4**, however, the N−B bond-stabilizing effect from catechol is absent. Instead, a chemical shift transition from sp^2 to sp^3 solvated boron centers was observed (see inset, Figure 14A), with an interconversion rate faster than the ^{11}B NMR time scale.[42,47]

The pH profiles of complexes between **4** and two other substrates — tetrafluorocatechol and fructose — were also examined. The decreased pK_{a1} compared to that of **4** for both complexes was evident, and the solvated complexes dominated the species distributions. However, the N−B coordinated species could not be unequivocally identified in either case.[80] Overall, the identification of an N−B coordinated species of **7** in an aqueous medium, albeit with a very small abundance, suggests that although the solvated species of arylboronates are dominant in aqueous media, the occurrence of the N−B coordinated species is still possible, and the abundance depends on the substrate and the solvent system.

3. Computational Analysis. To probe the nature of the N−B interaction further, we performed a series of calculations in a simulated water continuum. These calculations employed the Gaussian suite of programs using density functional theory (DFT) at the B3LYP/6-31+G(d,p) level of theory (see Supporting Information).

Optimized structures of relevant solution species in the association process of **4** and catechol were generated (Figure 15). The strength of N−B coordination in respective species should be reflected in their optimized geometries. The free receptor **4** displays a trigonal planar boronic acid moiety where the *o*-pyrrolidinylmethyl group extends away from the boronic acid moiety (Figure 15A). We further structurally restricted the geometries to bias the systems toward N−B coordination by orienting the pyrrolidinyl group nitrogen toward the boron atom. Once again, a distance of 2.7 Å between an sp^2 boron and pyrrolidinyl nitrogen was observed (Figure 15B), indicating negligible N−B coordination, even under biased conditions.

The structure of hydrated, zwitterionic compound **4** was optimized. Interestingly, one water molecule was eliminated and hydrogen-bonded between the sp^2-hybridized boronic acid and pyrrolidinyl moieties in the optimized structure (Figure 15C). The integrity of the zwitterionic structure was maintained only when the ammonium proton was restricted to facing directly away from the boronate site (Figure 15D).

Computational modeling of **4** with catechol to afford **7** results in an N−B bond length at 1.8 Å, accompanying a change in boron geometry from the trigonal planar as in the free boronic acid **4** to a tetrahedral for the boronate ester **7** (Figure 15E). The O−B−O bond angle in compound **4** is 117° (Figure 15A), well within the range for a stable trigonal planar structure. In comparison, the equivalent angle in the catechol boronate **7** is reduced to 107° (Figure 15E). The reduction in bond angle coupled with electron induction effect from the catechol substrate leads to a preferentially pyramidal boron atom. Furthermore, the O−B bond lengths increase from 1.38 Å in the free acid to 1.46 Å in the boronate ester, which indicates that donation from the nitrogen lone pair to the boron atom weakens back-donation from oxygen atoms. The O−B bond measurements in the computed structures are in agreement with the distances observed in single-crystal structures. The computed N−B bond formation is in agreement with our experimental conclusion that complexation with catechol promotes N−B coordination in aprotic solvents.

The hydrated, zwitterionic form of **7** was also modeled (Figure 15F). Unlike compound **4**, instead of elimination of a water molecule, the structure did not disintegrate, and a hydrogen bond was formed between the pyrrolidinium proton and the boronyl hydroxy group. The difference between hydrated **4** and **7** found by electronic structure theory supports our experimental conclusion that boronate ester formation stabilizes the solvated, zwitterionic boronate structures.

(76) James, T. D.; Shinkai, S. *Top. Curr. Chem.* **2001**, *218*, 159−200.
(77) Springsteen, G.; Wang, B. *Tetrahedron* **2002**, *58*, 5291−5300.
(78) Yoon, J.; Czarnik, A. W. *J. Am. Chem. Soc.* **1992**, *114*, 5874−5875.
(79) Shabbir, S. H.; Anslyn, E. V., unpublished results.

(80) For tetrafluorocatechol, the pK_{a1} and pK_{a2} are too different for the N−B bond formation to occur on a significant scale; for fructose, too many possible isomeric species of the complex impede the resolution of the ^{11}B NMR spectra.

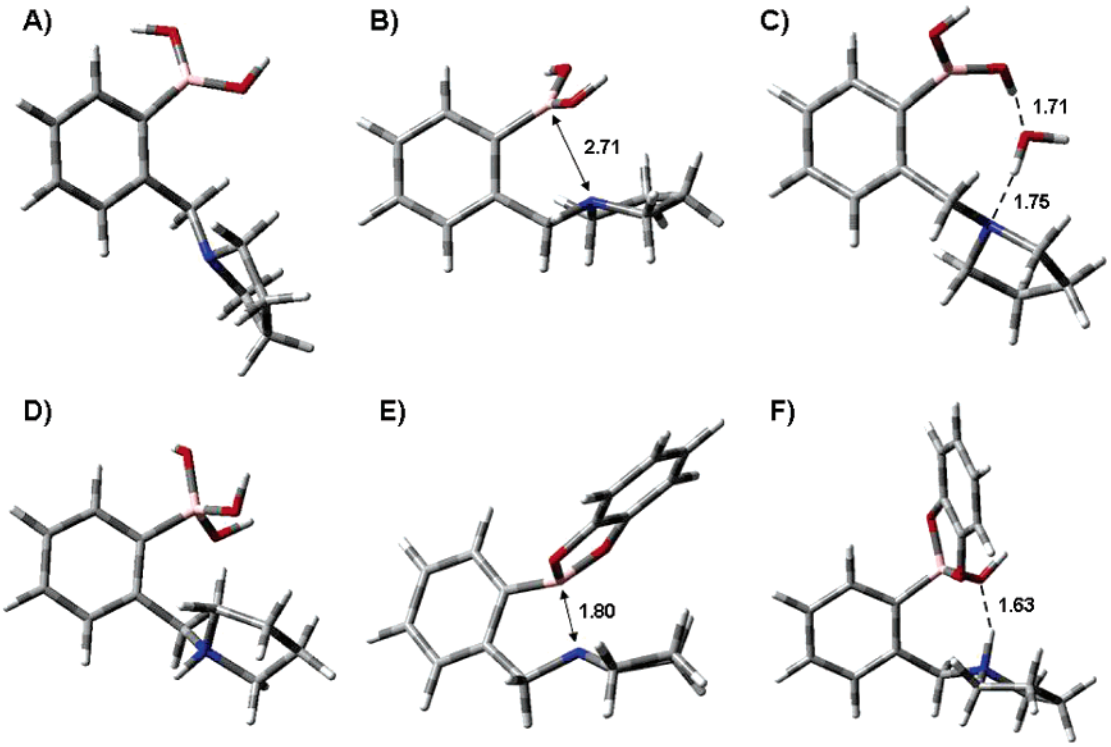

Figure 15. Energy-minimized structures (see text) of compound **4** (A,B), hydrated **4** (C,D), compound **7** (E), and hydrated **7** (F). The atomic distances are given in angstroms.

Conclusion

On the basis of our structural investigation, we first conclude that, in an aprotic solvent where the solvent insertion pathway is absent, an N−B dative bond is usually present in an *o*-(*N*,*N*-dialkylaminomethyl)arylboronate. However, in a protic media, solvent insertion of the boronate can dominate, which affords a hydrogen-bonded zwitterionic species with little or no N−B dative bond. Second, when a boronic acid associates with a vicinal bifunctionalized, electron-withdrawing substrate to afford a five-membered-ring cyclic boronate, both N−B bond formation and solvent insertion are promoted due to the increased electrophilicity/Lewis acidity of the boronate. The N−B coordinated and solvated species are in equilibrium. The abundances of the two species are decided by the relative strengths of the Brønsted acid/base interaction between an sp^2 boron and a protic solvent molecule and the Lewis acid/base interaction between the same boron atom and a neighboring nitrogen atom. Third, the first pK_a of an *o*-(*N*,*N*-dialkylaminomethyl)phenylboronate is primarily from hydroxylation of the sp^2 boronate, and the second pK_a is primarily from the deprotonation of the neighboring tertiary ammonium ion. The markedly lowered boronic acid acidity[33] compared to that of unsubstituted arylboronic acids (e.g., for phenylboronic acid p$K_a \approx 8.8$) is due to the ion-pairing stabilization from the neighboring tertiary ammonium ion. Last, the N−B coordinated species can be observed in small abundance, but their presence depends on their structures and the solvent.

By providing a relatively complete picture of the structures of *o*-(*N*,*N*-dialkylaminomethyl)phenylboronates, a widely used motif in molecular receptor and sensor design, the correct interpretations of available data can be achieved and the designs of future sensing technologies will be facilitated.

Acknowledgment. We thank Professors Seiji Shinkai, Tony D. James, and Binghe Wang for helpful suggestions. This study was supported by NIH (GM57306) and the Welch Foundation (F-1151).

Supporting Information Available: Experimental procedures, selected ^{11}B NMR spectra, and CIF files for all the single-crystal structures. This material is available free of charge via the Internet at http://pubs.acs.org.

JA055817C